

The crucial elements of the ‘last step’ of programmed cell death induced by kinetin in root cortex of *V. faba* ssp. *minor* seedlings

Magdalena Doniak · Mirosława Z. Barciszewska ·
Joanna Kaźmierczak · Andrzej Kaźmierczak

Received: 14 April 2014/Revised: 25 August 2014/Accepted: 1 September 2014/Published online: 12 September 2014
© Springer-Verlag Berlin Heidelberg 2014

Abstract

Key message Kinetin-induced programmed cell death, manifested by condensation, degradation and methylation of DNA and fluctuation of kinase activities and ATP levels, is an autolytic and root cortex cell-specific process.

Abstract The last step of programmed cell death (PCD) induced by kinetin in the root cortex of *V. faba* ssp. *minor* seedlings was explained using morphologic (nuclear chromatin/aggregation) and metabolic (DNA degradation, DNA methylation and kinases activity) analyses. This step involves: (1) decrease in nuclear DNA content, (2) increase in the number of 4',6-diamidino-2-phenylindole (DAPI)-stained chromocenters, and decrease in chromomycin A₃ (CMA₃)-stained chromocenters, (3) increase in fluorescence intensity of CMA₃-stained chromocenters, (4) condensation of DAPI-stained and loosening of CMA₃-stained

chromatin, (5) fluctuation of the level of DNA methylation, (6) fluctuation of activities of exo-/endonucleolytic Zn²⁺ and Ca²⁺/Mg²⁺-dependent nucleases, (7) changes in H1 and core histone kinase activities and (8) decrease in cellular ATP amount. These results confirmed that kinetin-induced PCD was a specific process. Additionally, based on data presented in this paper (DNA condensation and ATP depletion) and previous studies [increase in vacuole, increase in amount of cytosolic calcium ions, ROS production and cytosol acidification “in Byczkowska et al. (Protoplasma 250:121–128, 2013)”], we propose that the process resembles autolytic type of cell death, the most common type of death during development of plants. Lastly, the observations also suggested that regulation of these processes might be under control of epigenetic (methylation/phosphorylation) mechanisms.

Keywords ATP · Cell death · Chromatin condensation · Kinase activities · Methylation of DNA · Nuclease activities · Root cortex cells

Communicated by Prakash P. Kumar.

M. Doniak · A. Kaźmierczak (✉)
Department of Cytophysiology, Faculty of Biology and
Environmental Protection, University of Łódź,
Pomorska 141/143, 90-236 Łódź, Poland
e-mail: kazand@biol.uni.lodz.pl

M. Doniak
e-mail: magdadoniak@o2.pl

M. Z. Barciszewska
Institute of Bioorganic Chemistry, Polish Academy of Sciences,
Noskowskiego 12/14, 61-704 Poznań, Poland
e-mail: Mirosława.Barciszewska@ibch.poznan.pl

J. Kaźmierczak
School of Polish for Foreigners, University of Łódź,
Matejki 21/23, 90-231 Łódź, Poland
e-mail: jokazm@interia.pl

Introduction

Programmed cell death is a genetically regulated “sequence of (potentially interruptible) events” (Reape et al. 2008) in both plant and animal organisms (Gladish et al. 2006) that leads to cell degradation (Gunawardena 2008). In animals, PCD is recognised as apoptosis, autophagy or necrosis while in plants categorization of cell death is not unequivocal. That is why Galluzzi et al. (2007) and then van Doorn et al. (2011), according to recommendations of the Nomenclature Committee on Cell Death 2009 (Kroemer et al. 2009), proposed to apply morphological criteria to categorise animal and plant cell deaths,

respectively. It seems that only animal cell death is exactly categorised (Kroemer et al. 2009). In plants vacuolar, necrotic and mixed (atypical) forms of programmed cell death were recognized on the basis of the presence of lytic vacuoles (van Doorn et al. 2011). In the vacuolar type of death, vacuoles grow by fusion with small cellular vesicles, lytic vacuoles collapse and release hydrolases which gradually digest entire or most of the contents of terminally differentiated cells excluding cell walls (Bollhöner et al. 2012). Metacaspases (e.g. mCII-Pa), cysteine proteases distantly related to caspases, are required in this type of cell death (Minina et al. 2013). In the necrotic one there are no vacuolar cell death features while the early rupture of plasma membrane and shrinkage of protoplast can be observed (van Doorn et al. 2011). Normal development of plant organisms, i.e. tissue and organ formation or their elimination as well as nutritional stress, are accompanied with vacuolar type of death, while accidental or injury-induced cellular demise due to physical destruction of the cellular integrity triggers necrotic processes (Reape et al. 2008; van Doorn et al. 2011). To distinguish necrosis, non-programmed type of death, from the similar, but programmed one (McCall 2010), the “necroptosis” name was introduced (Kroemer et al. 2009). Types of plant cell death classified by van Doorn et al. (2011) as mixed or atypical are expressed during hypersensitive responses (HR) to pathogens, in starchy cereal endosperm and during self-incompatibility.

Comparison of metabolic hallmarks of animal and plant cell deaths allowed van Doorn (2011) to propose another classification system which includes two classes of cell death: “autolytic” and “non-autolytic”. It is important that this classification is dedicated to processes that occur in intact plants but not in cell cultures (van Doorn 2011). The autolytic type of death, generally occurs after rupture of a tonoplast and it leads to leakage of vacuole contents which is observed as rapid clearance (it is evoked by the dilution by vacuolar contents) of cytoplasm. There are condensation and aggregation of chromatin, movement of condensed chromatin to the periphery of a nucleus, condensation of the nuclei to smaller diameters and their breakup into small fragments, increase in vacuolar volume and also swelling of organelles. According to van Doorn (2011), autolytic cell death includes death occurring during developmental steps of plant organisms e.g. male and female gametophytes as well as xylem conduits (Pennell and Lamb 1997) and bark formation, senescence (Pennell and Lamb 1997) of leaves and petals as well as development and germination of seeds (Pennell and Lamb 1997; van Doorn and Woltering 2005) as well as during hypoxia and plant pathogen interactions (Pennell and Lamb 1997). This type of death is accompanied by increase in cytoplasmic calcium ion concentrations (Bosch et al. 2008; Kunikowska

et al. 2013a), induction of MAPK (mitogen activated protein kinase) signalling, acidification of cytosol, changes in microtubule and actin cytoskeleton (Bosch et al. 2008). Autolytic cell death is also manifested by degradation of macromolecules such DNA, RNA, lipids, carbohydrates (also these in a cell wall; Gunawardena 2008) and proteins (van Doorn 2011). Metabolites of their degradation are transported via phloem into developing organs e.g. grains (Gregersen et al. 2008). Autolytic cell death often requires serine and/or cysteine proteases and changes in the nucleus occurring only after tonoplast rupture (Obara et al. 2001), closure of the plasmodesmata (van Doorn et al. 2003) and early depletion of ATP level (Azad et al. 2008). The non-autolytic cell death, which looks like necrotic cell death type (van Doorn and Woltering 2005), where tonoplast rupture does not occur or where tonoplast rupture is not followed by complete clearance of the cytoplasm, is mainly found during PCD due to plant–pathogen interactions, e.g. HR as well as during the PCD in endosperm in cereal seeds (van Doorn 2011). It seems that both vascular and autolytic cell death include the cell death recognized as autophagic (van Doorn and Woltering 2005; Minina et al. 2013).

Condensation and aggregation of chromatin, transition of condensed chromatin to the nucleus periphery, condensation of a nucleus to a smaller diameter or its breakup into small fragments and then its degradation are the first hallmarks of the final step of cell degradation (Domínguez and Cejudo 2012). Because these hallmarks are similar to those observed during apoptosis (Kroemer et al. 2009), existence of apoptotic-like cell death in plants is proposed (Carimi et al. 2003; Gladish et al. 2006; Reape et al. 2008). This type of cell death concerns only dividing cells present in cell culture systems (Carimi et al. 2003; Reape et al. 2008), in procambium as well as in ground meristem as it was observed in pea (*Pisum sativum*) root tips after their exposure to sudden flooding (Gladish et al. 2006).

It was reported that kinetin induced cell death in root cells of *V. faba* ssp. *minor* seedlings (Kunikowska et al. 2013a). This death was initially classified as kinetin-specific vacuolar type of cell death (Kunikowska et al. 2013a), however, some features of this process pointed to an autolytic type. Taking into account this fact, it was important to conduct studies to dispel the doubts about the type of kinetin-induced cell death. Thus, this study was focused on the nucleus degradation, a common step for animal and plant cell death (van Doorn 2005; Domínguez and Cejudo 2012). In this study, 3-day-old *V. faba* ssp. *minor* seedlings, treated with kinetin, were used to estimate nuclear chromatin condensation/aggregation, DNA degradation, DNA methylation and kinase activities. Previous results (Kunikowska et al. 2013a) allowed us to suggest that 72-h treatment with kinetin was probably the “culmination point” of root cortex cell death induced by

kinetin, since the number of dying cells after 72-h of treatment with kinetin was higher than after 96 h (Kunikowska et al. 2013a). In the present research, analyses were also carried out 24 h before and after this point, i.e. 48 and 96 h after kinetin treatment.

Materials and methods

Material, treatment and analyses

To study the PCD process, 20 seeds of *V. faba* ssp. *minor* were dark germinated in breeding chamber at 23 °C in Petri dishes (15 cm diameter and 3 cm height) on blotting paper moistened with distilled water (2 ml per seed) for 3 days. Then six of the 3-day-old *V. faba* ssp. *minor* seedlings with almost equal length (2.5 ± 0.2 cm) of roots were transferred to a glass container (8 cm diameter and 4 cm height) with blotting paper moistened with 10 ml of kinetin solution (46 μM) and cultivated in the two experimental systems at 23 °C in the dark with 92 % of humidity.

The first experimental system consisted in 3-day-old *V. faba* ssp. *minor* seedlings cultivated with water for 72 h without (72-h Ctrl; control) or with kinetin (72-h kinetin treated). Roots of these seedlings were used to determine (1) the nuclear profile area (NPA), (2) the content of nuclear DNA expressed in arbitrary units of fluorescence intensity (au of FI) after DAPI staining and, (3) the nuclear chromatin condensation of cortex cells as well as (4) the electrophoretic profiles of human and faba bean DNA degraded with acidic and basic nucleases extracted from 2 cm long apical parts (without meristem) of *V. faba* ssp. *minor* seedling roots.

The second experimental system consisted in 3-day-old seedlings (T0 Ctrl, initial control) subsequently treated with kinetin for 48, 72 and 96 h. The 2 cm long apical parts of roots of these seedlings (without meristems) were used to measure (5) the actual (spectrophotometrically measured) DNA content, (6) DNA methylation, (7) ATP amount and (8) kinase activities with core and H1 histones as substrates.

For all cytomorphologic and analytic experiments, the 2-cm long apical parts of root fragments without meristems (i.e. between 4 and 20 mm from the root tip) were used because PCD was observed there.

Cell death and microcytophotometric DNA content as well as NPA and chromatin condensation estimation

To confirm cell death existence in *V. faba* ssp. *minor* seedling roots after kinetin treatment, the “double staining method” described in Byczkowska et al. (2013) was

applied. In situ analyses of the cell death were carried out only in the cortex cells between the 4th and the 20th mm of 2 cm long apical parts of two or three roots from three independent experiments. The “double staining method” is based on the measurement of resultant fluorescence intensity (RFI) of green AO (acridine orange; Sigma), migrating into the nuclei via cellular membranes even if its permeability is not increased, and red EB (ethidium bromide; Sigma), permeating only to dying or dead cells in which cellular membranes permeability increases. The colour of chromatin of cells undergoing PCD is green-yellow, yellow or yellow-orange, reflected in greater RFI values, then in green (living) cells. The colour of chromatin of dead cells is dark orange and red and in these nuclei RFI values reach the highest levels (Byczkowska et al. 2013). It allows us to distinguish living, dying and dead cells. Detection of cell death was carried out according to the procedure described in Byczkowska et al. (2013), in particular, by staining the roots with the mixture of 100 $\mu\text{g ml}^{-1}$ acridine orange (AO) and 100 $\mu\text{g ml}^{-1}$ EB in PHB (0.01 M phosphate buffer, pH 7.4) for 4 min and fixing them with 1.0 % glutardialdehyde (POCH, Poland) in PHB for 15 min. Then the roots were cut with a razor blade along the long axis and thin sections, washed two times for 2 min with PHB, were put on glass slides with a drop of PHB, covered with coverslip and analysed (Byczkowska et al. 2013). To detect cell death, the fluorescence micrographs from the specimens placed on slides were taken under blue (400–440 nm of B-2A excitation filter) light using the Optiphot-2 epifluorescence microscope (Nikon) equipped with DDX camera and Act1-software (Precoptic, Poland). To estimate the numbers of living, dying and dead cells, the RFI of OA/BE was measured using the ScnImage software according to the procedure described in Byczkowska et al. (2013) on the basis of 150–200 nuclei from each of three independent experiments.

Microcytophotometric DNA content and NPA were estimated in cortex cells of 2 cm long apical parts of 2 or 3 roots without meristems from three independent experiments of 72-h Ctrl and 72-h kinetin-treated *V. faba* ssp. *minor* seedlings, which were fixed in cold Carnoy's (96 % ethanol and glacial acetic acid; 3:1) for 1 h and then washed with 96 and 70 % ethanol, hydrated and stained with 0.2 $\mu\text{g ml}^{-1}$ of 4,6-diamidino-2-phenylindol (DAPI; Sigma) according to the procedure developed by Kaźmierczak (2010). The roots were pretreated with 0.2 M citric acid and 0.1 % Tween, stained with DAPI (2 $\mu\text{g ml}^{-1}$) mixed with 0.1 M Na_2HPO_4 and 0.2 M citric acid in 9:1 ratio for 5 min. After 5 min washing with the mixture of Na_2HPO_4 and citric acid, the roots were cut with a razor blade along the long axis onto very thin sections, washed twice with PHB, put on glass slides with a drop of PHB and analysed. To estimate microcytophotometric

DNA content, the micrographs from the specimens placed on slides were taken under UV light (330–400 nm UV-2A excitation filter) using the epifluorescence microscope. Next they were used to measure fluorescence intensity (FI) with the ScnImage software (Byczkowska et al. 2013) on the basis of 400–500 nuclei from each of three independent experiments. Values of FI of nuclei after DAPI staining were used to prepare histograms from which average of total DNA content per one nucleus and the distribution of cells with >2, 2, 2–4, 4 and >4C DNA were estimated. The same micrographs were also used to measure nuclear profile area of whole nuclei using the ScnImage software.

Estimation of chromatin condensation was done in the nuclei of root cortex cells of 72-h Ctrl and 72-h kinetin-treated seedling roots by counting the number of chromocenters per one nucleus after DAPI and CMA₃ staining. Staining with CMA₃ was performed similarly as with DAPI but 20 µg ml⁻¹ of CMA₃ with 20 mM MgCl₂ were used. Fluorescence micrographs from the specimens placed on slides were taken under blue (400–440 nm B-2A excitation filter) light and 150 nuclei of three independent experiments with similar NPA ($P > 0.05$; at about 146 µm²) and with similar DNA content (cytrophotometrically estimated post-DAPI), corresponding to about 4C values (about 2,800 au of FI), were analysed. In this experiment, chromatin condensation per one unit of nucleus profile area (expressed in percent) was also estimated on basis of fluorescence intensity (expressed in au). The amount of fluorescence intensity on Fig. 6 means the area indicated between y axis (% of nuclei area) and x axis (level of fluorescence intensity) of particular data line. The amount of fluorescence levels of DAPI- or CMA₃-stained chromatin intensity above 50 % of the nuclear profile means condensed part of chromatin while that under 50 % means uncondensed one.

DNA preparation for estimation of its methylation and actual content and nuclease degradation profile

DNA extraction from the apical fragments of roots (without meristems) of T0 Ctrl *V. faba* ssp. *minor* seedlings and of those treated with kinetin for 48, 72 and 96 h was carried out on ice with 2 % SDS, 0.5 M NaCl, 100 mM Tris-HCl and 50 mM EDTA at pH 8.0. Homogenates were incubated and vortexed at 65 °C for 40 min, chilled on ice with 200 µl of 5 M potassium bi-sulphite for 10 min to decrease the protein content in the samples, and centrifuged (5,000g for 10 min) at 4 °C. Then, 1.0 volume of chloroform/isoamyl alcohol (24:1) was added to the samples, vigorously mixed and centrifuged (5,000g at 4 °C) for 10 min. The upper phase, containing DNA, was transferred to a fresh tube and then extracted with 0.8 volume of cold isopropanol. The pellets were washed twice with 70 %

ethanol, microcentrifuged for 1 min, dried, and re-suspended in TE buffer (1 mM Tris-HCl, pH 8.0, and 1 mM EDTA, pH 8.0) with 20 µg ml⁻¹ RNase A at 25 °C (Byczkowska et al. 2013). These samples, after spectrophotometric measurements of actual DNA content, were used to study its methylation. Spectrophotometric determination of DNA content was done by mixing 1–2 µl of each sample containing extracted DNA with 2 ml of TE buffer and absorbance at 260 nm using Ultrospec 1100 pro spectrophotometer was measured. The amount of DNA was calculated using the rule indicating that absorption of 50 nM of DNA at 260 nm is equal to 1 unit of optical density (OD) based on three independent experiments in three replicates.

Analyses of DNA profile degradation

Nucleases were extracted from apical fragments of 72 h Ctrl and 72-h kinetin-treated *V. faba* ssp. *minor* seedling roots. The roots were weighed and frozen on solidified carbon dioxide in Eppendorf tubes and homogenised on ice in these tubes using the glass pestle with the 0.05 M Tris-HCl at pH 7.0 buffer (200 µl per 100 mg of FW of tissue) and then they were centrifuged (5,000g at 4 °C) for 10 min. The pellets were extracted once again in a similar manner. 10 µl of the combined supernatants containing nucleases were mixed with 10 µg samples of human (Sigma) or faba bean (prepared by the authors from T0 Ctrl seedlings) DNA. The activity of acidic nucleases was estimated with 0.2 M acetate pH 5.5 buffer containing 1 mM ZnCl₂ while that of basic ones with 5 mM Tris-HCl pH 7.5 buffer containing 5 mM MgCl₂ and 5 mM CaCl₂. Digestion was carried out for 30 min at 37 °C. After digestion, the samples were supplemented with 1.0 volume of chloroform/isoamyl alcohol (24:1), vigorously mixed and centrifuged (5,000g at 4 °C) for 10 min. The upper phase containing DNA was transferred to a fresh tube and extracted by 30 min with 0.8 volume of cold isopropanol alcohol at -20 °C. After next centrifugation the pellet was supplemented with 300 µl of 70 % ethanol, centrifuged for 1 min, dried and re-suspended in TE buffer.

DNA samples and DNA marker (1 kb DNA Ladder, 250–10,000 bp, Fermentas) were simultaneously separated at 100 V for 2–2.5 h on a 1.0 % (w/v) agarose gel and then stained with 0.50 µg ml⁻¹ EB and photographed.

Estimation of DNA methylation

The level of methylated deoxycytosine (m⁵dC) was estimated in the DNA extracted from the apical fragments (without meristem) of T0 Ctrl *V. faba* ssp. *minor* seedling roots and from those treated for 48, 72 and 96 h with kinetin.

Analyses were carried out with two-directional TLC chromatography on cellulose (Merck) plates with [^{32}P] m^5dC according to Barciszewska et al. (2007) after the samples of DNA were digested with spleen phosphodiesterase II and micrococcal nuclease at 37 °C and labelled with [^{32}P]ATP (ICN) and T4 polynucleotide kinase. Analyses were made on Phosphoimager Typhoon (Pharmacia) with Image Quant Software. Calculations of the m^5dC amount (%) were done in relation to deoxypyrimidines (dC and dT).

Determination of ATP content and kinase activities

ATP amount and kinase activities were determined in extracts from apical parts (without meristems) of roots of T0 Ctrl *V. faba* ssp. *minor* seedlings and those treated with kinetin for 48, 72 and 96 h. The extracts were obtained in the similar manner like nucleases with the buffer containing 40 mM Tris (pH 7.4), 20 mM MgCl_2 , 10 $\mu\text{g ml}^{-1}$ BSA (bovine serum albumine) and 1 mM PMSF (phenylmethylsulfonyl fluoride; Sigma). After centrifugation for 10 min at 5 000 g (4 °C), the pellets were extracted once again and centrifuged for 10 min (4 °C). The combined supernatants were used to measure the amount of ATP and protein kinase activities with a Kinase-Glo Luminescent Kinase Assay Kit (Promega) containing Kinase-Glo Buffer and the lyophilized Kinase-Glo Substrate (thermostable UltraGlow Recombinant Luciferase).

To estimate the amount of ATP in the extracts the luminescence was measured in the samples supplemented with the extraction buffer, Kinase-Glo reagent. ATP amount was presented in relative luminescence units (RLU) calculated per 1 g of FW of roots.

The reaction mixture to estimate kinase activities in the tested samples was prepared with, sequentially added, 20 μl of the extract from 2 cm long apical part of roots, 1,035 μl extraction buffer, 5 μl of ATP, 20 μl (2 $\mu\text{g ml}^{-1}$) core (Sigma) or 10 μl (2 $\mu\text{g ml}^{-1}$) H1 histones (Sigma) as substrates and 50 μl of Kinase-Glo reagent. After mixing, the luminescent signals were measured by fluorescence/luminescence spectrophotometer F-2500 (Hitachi) at 458 nm every 30 s for 2.5 min. The kinase activities were calculated as the difference between the luminescence of the samples without H1 or core histones (reference sample) and the luminescence of the amount of ATP not used for histone phosphorylation by kinases in the tested samples. The unit of kinase activities was expressed in RLU as a amount of ATP used by kinases per 1 g of FW of roots.

Statistical analysis

The results of cytomorphological research were statistically verified using the Student's *t* test while the results of metabolic research were verified by Mann–Whitney *U* test

and the *P* value were applied to indicate significance of differences between the results.

Results

DNA content and size of nuclei

NPA of root cortex cell nuclei of *V. faba* ssp. *minor* seedling roots was measured after DAPI staining of the 72-h Ctrl roots. It was showed that in the roots treated with kinetin for 72 h NPA was greater by about 40 % then in Ctrl (Fig. 1a). Whereas the total DNA content in the nuclei estimated by microcytophotometric measurements, expressed in au of DAPI FI was significantly ($P < 0.05$) lower, by about 30 % in 72-h kinetin-treated seedling roots as compared to 72-h Ctrl ones (Fig. 1b).

DNA content expressed in C values after microcytophotometric measurement of DAPI FI showed that the 72-h treatment with kinetin changed the number of root cortex cells with 2, 2–4, 4 and >4C (endo phase) DNA compared to the 72-h Ctrl roots. The number of 2, 4 and >4C cells was lower by about 11.5, 1 and 1 %, respectively, whereas the number of 2–4 C cells was greater by about 2.5 % (Fig. 2).

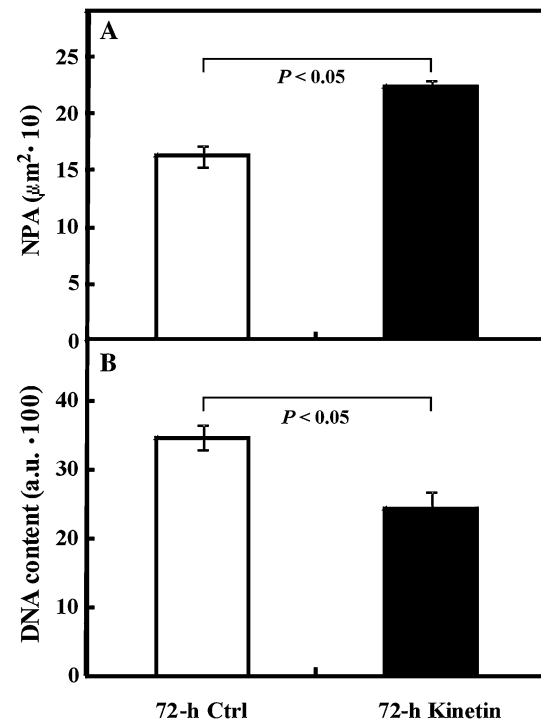


Fig. 1 Nuclear profile area (a) and cytophotometrically determined DNA content (b) in the nuclei of cortex cells of 2 cm apical parts of 72-h Ctrl and 72-h kinetin-treated of *V. faba* ssp. *minor* seedling roots. Error bars represent the SE on the mean of three experiments ($n = 450$). $P < 0.05$ indicates statistically significant differences between the neighbouring results

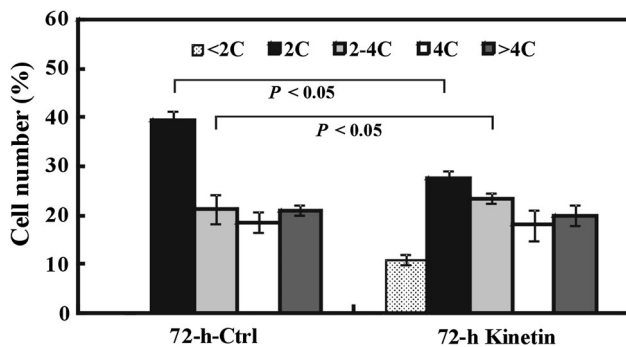


Fig. 2 Number of 2, 2–4, 4C, endoreplicated (>4C DNA) and hypoploid (<2C) cells microcytphotometrically determined in cortex of 72-h Ctrl and 72-h kinetin-treated 2 cm apical parts of *V. faba* ssp. *minor* seedling roots after DAPI staining. Error bars represent the SE of the mean of three independent experiments ($n = 450$). $P < 0.05$ indicates statistically significant differences between the results marked by line

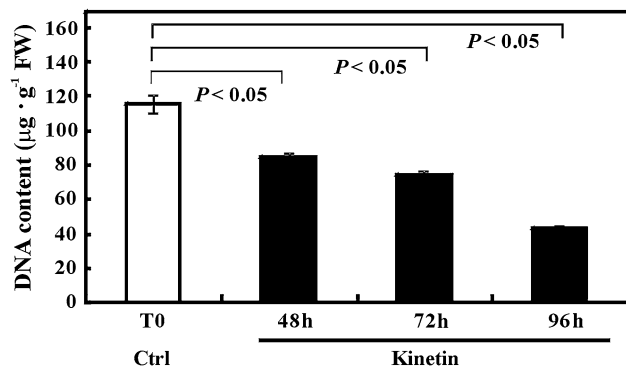


Fig. 3 Content of spectrophotometrically determined DNA in the 2 cm apical parts of T0 Ctrl and after 48, 72 and 96 h treatment with kinetin *V. faba* ssp. *minor* seedling roots. Error bars represent the SE on the mean of three experiments ($n = 3$). $P < 0.05$ indicates statistically significant differences between the results marked by line

Additionally, the fraction (11.0 %) of nuclei with DNA content less than 2C (hypoploid cells) appeared (Fig. 2). Significant differences ($P < 0.05$) in the number of cells between the control and the kinetin-treated roots were noted for the cells with 2 and 2–4C DNA content.

Spectrophotometric measurements of DNA content (real DNA content) extracted from the apical parts of roots showed that 1 g of FW of T0 Ctrl roots contained about $120 \pm 5.2 \mu\text{g}$ of DNA. In the seedlings treated with kinetin for 48, 72 and 96 h, DNA contents were significantly ($P < 0.05$) lower by about 26, 36 and 64 %, respectively (Fig. 3).

Chromatin condensation

The nuclei of root cortex cells of 72-h Ctrl and 72-h kinetin-treated seedlings with similar NPA and cytophotometrically

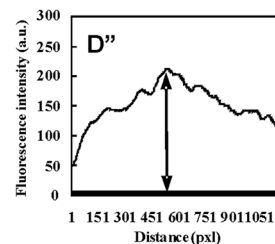
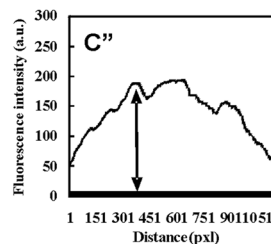
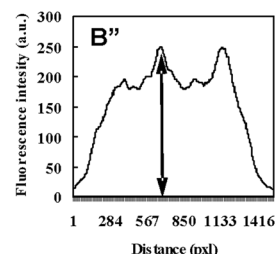
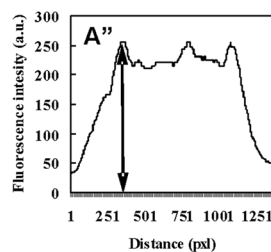
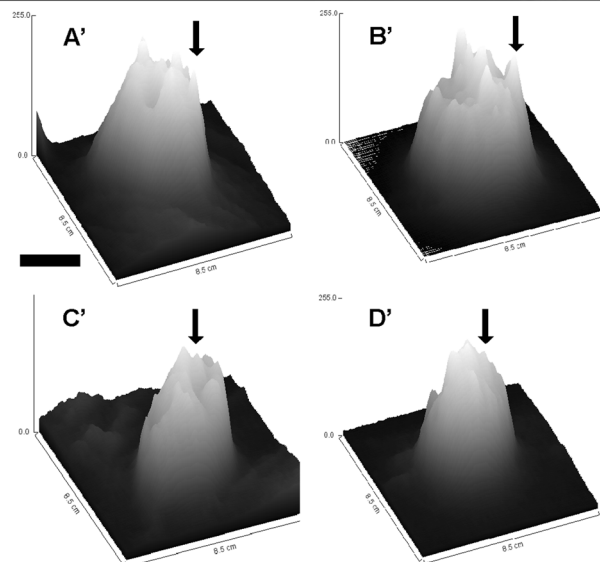
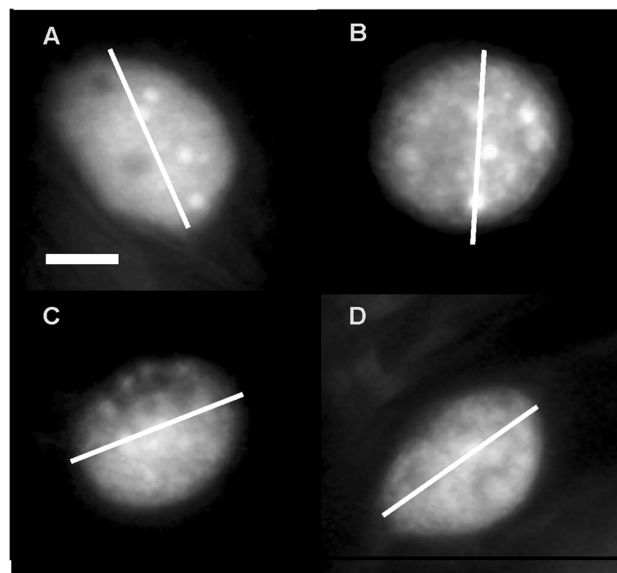


Fig. 4 Nuclear chromocenters with surface and fluorescence line plot profiles of the nuclei of cortex cells after DAPI (a, b; a', b'; a'', b'') and CMA₃ (c, d; c', d'; c'', d'') staining of 72-h Ctrl (a, c; a', c'; a'', c'') and 72-h kinetin-treated (b, d; b', d'; b'', d'') 2 cm apical parts *V. faba* ssp. *minor* seedling roots. Bars in a, a' = 10 μm and are applied in a-d and a'-d'

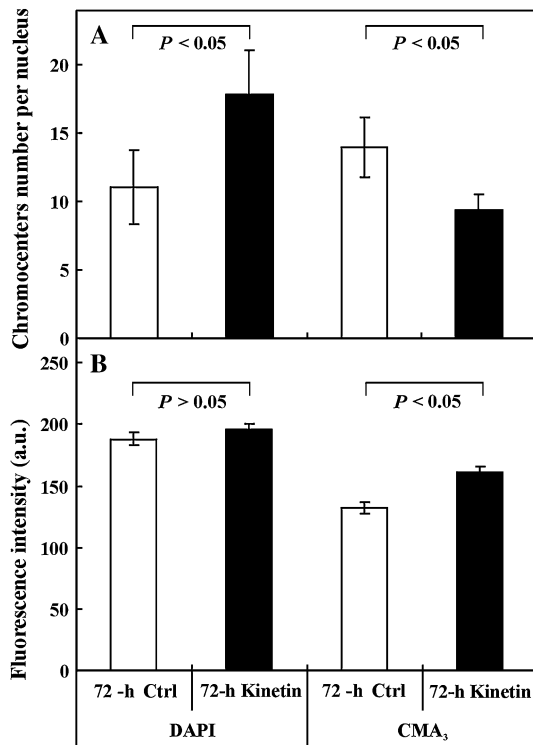


Fig. 5 Number of chromocenters (a) and values of their fluorescence intensity (b) in DAPI and CMA₃ stained nuclei of root cortex cells of 72-h Ctrl and 72-h kinetin-treated *V. faba* ssp. *minor* seedlings. Error bars represent the SE on the mean of three experiments ($n = 150$). $P < 0.05$ indicates statistically significant, while $P > 0.05$ indicates statistically insignificant differences between the results marked by line

estimated DNA contents were studied to assess chromatin condensation after DAPI (Fig. 4a, b) and CMA₃ (Fig. 4c, d) staining by counting the number of chromocenters and by measuring their values of fluorescence intensity of the plot line profiles as well as by examining the amount of condensed and uncondensed chromatin, which was expressed in values of FI per units of nuclear profile area expressed in percent.

The number of chromocenters in DAPI-stained nuclei (Fig. 5a), which was counted digitally per nucleus using their surface plot profile (Fig. 4a, a', b, b') was greater in 72-h kinetin-treated roots by about 7 ($P < 0.05$) compared to 72-h Ctrl roots (Fig. 5a). In the nuclei stained with CMA₃ (Fig. 4c, d), the number of chromocenters in 72-h kinetin-treated roots (Fig. 4d, d') was lower by about 5

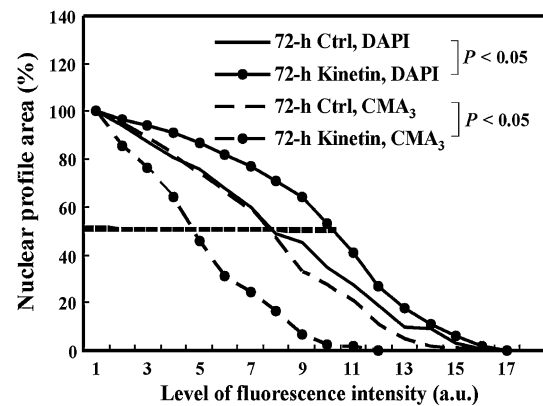


Fig. 6 Nuclear profile areas of 4C nuclei versus their fluorescence intensity after DAPI and CMA₃ staining in the root cortex cells of 72-h Ctrl and 72-h kinetin-treated *V. faba* ssp. *minor* seedlings. Dotted line indicates the 50 % surface of nucleus ($n = 150$ of each of three experiments). $P < 0.05$ indicates statistically significant differences between the results marked by line

($P < 0.05$) per nucleus (Fig. 5a) compared to 72-h Ctrl roots (Fig. 4c, c'). However, the maximal value of plot profile of fluorescence intensity of DAPI-stained (Fig. 4a', b'') chromocenters was about 188.0 ± 16 au in 72-h Ctrl roots and was similar ($P > 0.05$, 196 au) to this in 72-h kinetin-treated roots (Fig. 5b), while the FI of CMA₃-stained (Fig. 4c'', d'') chromocenters was about 132.0 ± 19.0 in 72-h Ctrl roots while in 72-h kinetin-treated roots it was significantly ($P < 0.05$) greater and it was 161.0 ± 14.0 au (Fig. 5b).

Part of chromatin of nuclei, stained with DAPI, expressed per unit of area of these nuclei (Fig. 6) showed that chromatin in the nuclei of 72-h Ctrl roots was condensed in about 45 % of au of fluorescence intensity while in 72-h kinetin-treated material this value was significantly ($P < 0.05$) greater by about 10 %. Whereas, the values of fluorescence intensity of CMA₃-stained part of chromatin per unit of area of nuclei of 72-h Ctrl roots were about 42 % of au of fluorescence intensity of whole chromatin and in the kinetin-treated material (Fig. 6) this values were significantly ($P < 0.05$) lower by about 10 %.

DNA methylation

DNA methylation level expressed by the percentage of m⁵dC in the plant material extracted from the apical part of T0 Ctrl *V. faba* ssp. *minor* seedling roots was about 6.5 % (Fig. 7). While in those treated with kinetin for 48, 72 and 96 h the levels of m⁵dC compared to T0 Ctrl were lower by about 0.7 %, greater by about 0.5 and 1.0 %, respectively (Fig. 7). Differences in the levels of DNA methylation between T0 Ctrl and 48 h of kinetin treatment as well as between 48 and 72 h were statistically significant

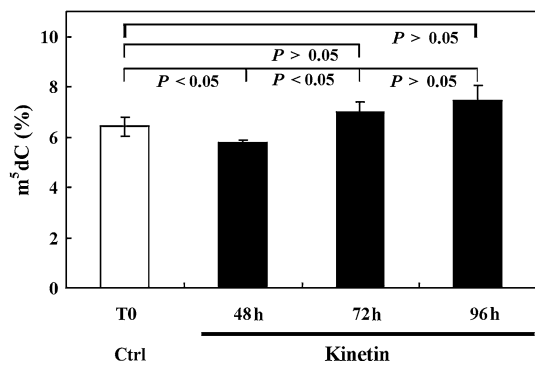


Fig. 7 Level of m⁵dC in DNA extracted from the 2 cm apical parts of roots of T0 Ctrl and after 48, 72 and 96 h treatment with kinetin of *V. faba* ssp. *minor* seedlings. Error bars represent the SE on the mean of two experiments ($n = 3$). $P < 0.05$ and $P > 0.05$ indicate statistically significant or insignificant differences, respectively, compared to T0 Ctrl and between the results marked by line

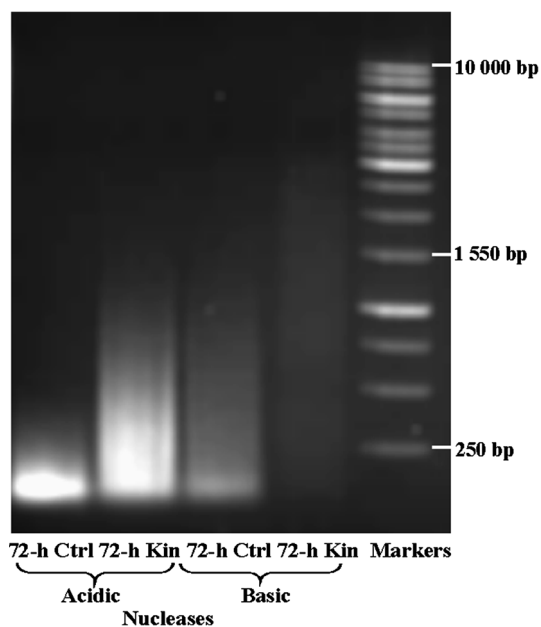


Fig. 8 Electrophoretogram of human DNA digested for 30 min with acidic (line 1, 2; from the left side) and basic (line 3, 4; from the left side) nucleases from the 2 cm apical parts of 72-h Ctrl and 72-h kinetin-treated *V. faba* ssp. *minor* seedling roots and DNA markers (250–10,000 bp)

($P < 0.05$) whereas differences between 72 and 96 h treatment were not statistically significant ($P > 0.05$).

Profiles of DNA digestion

Human and faba bean DNA digested by nucleases extracted from 2 cm apical parts of 72-h Ctrl and 72-h kinetin-treated of *V. faba* ssp. *minor* seedling roots were electrophoretically separated on the agarose gel (Figs. 8, 9).

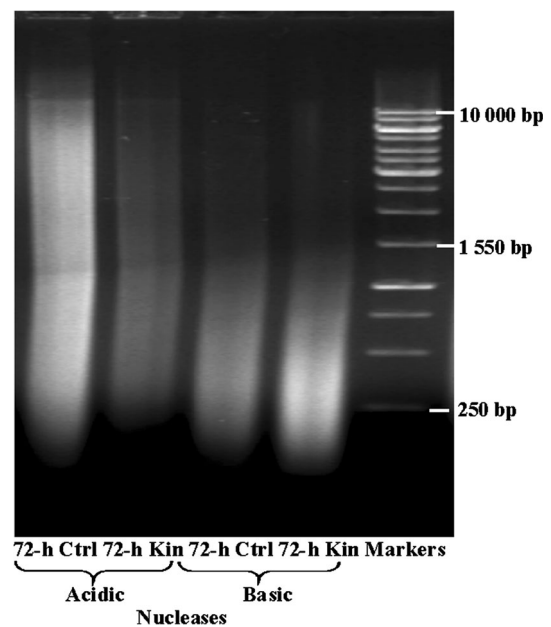


Fig. 9 Electrophoretogram of faba bean DNA digested for 30 min with acidic (line 1, 2; from the left side) and basic (line 3, 4; from the left side) nucleases of the 2 cm apical part of 72-h Ctrl and 72-h kinetin-treated *V. faba* ssp. *minor* seedling roots. Line 5 presents DNA markers (250–10,000 bp)

The results showed that human DNA was hydrolysed by acidic and basic nucleases from 72-h Ctrl roots into fragments ranging from 500 to <250 and 1,500 to <250 bp in length (Fig. 10), respectively, with its maximum density below 250 bp (Fig. 10b, c). Kinetin treatment changed the activity of these nucleases, and the acidic nucleases generated fragments between 2000 and <250 bp with its maximum density, expressed in values of FI, below 250 bp while the basic nucleases degraded human DNA into 3000 to <250 bp fragments in length with its maximum density at 750 bp. Moreover, their maximum density from the kinetin-treated samples after kinetin treatment was lower than in 72-h Ctrl roots by about 40 % in acidic and 80 % in basic nucleases (Fig. 10d, e) indicating increase in their activity.

Faba bean DNA digestion by the acidic and basic nucleases (Fig. 11) in 72-h Ctrl generated DNA fragments between 10 000 and 250 bp with maximum density at 2,500 and 750 bp and fragments between 1,500 and 250 bp with their maximum density at 500 and 250 bp, respectively (Fig. 11b, c). Kinetin treatment did not change general length of released fragments but it changed their maximum density. Densities of fragments generated by acidic nucleases from 72-h kinetin-treated roots were lower by about 40 %, indicating higher activities of nucleases while the maximum densities of DNA fragments generated by basic nucleases were greater by about 20 % (Fig. 11d, e), indicating their lower activity.

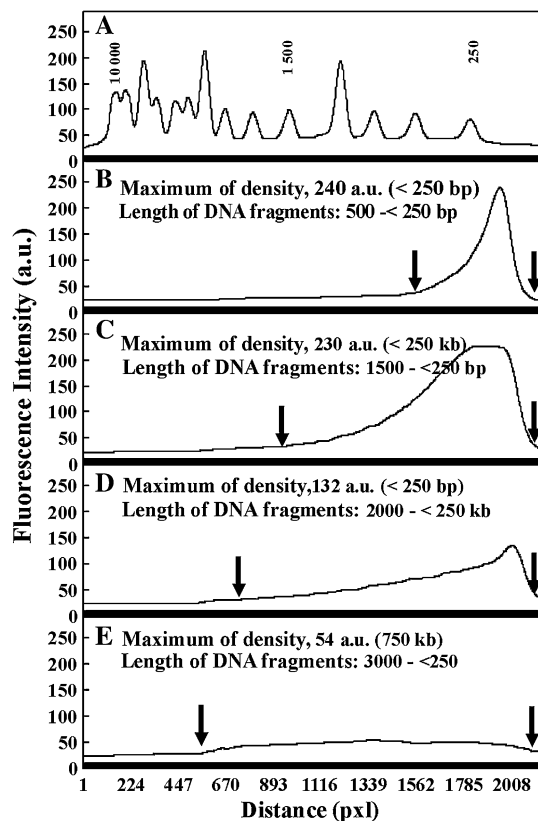


Fig. 10 Densitometric plot of fluorescence intensity of electrophoresed DNA markers (a) and human DNA digested for 30 min with acidic (line b, c) and basic (line d, e) nucleases isolated from the 2 cm apical parts of 72-h Ctrl (b, d) and 72-h kinetin-treated (c, e) of *V. faba* ssp. *minor* seedling roots. Arrows indicate electrophoresed DNA fragments

ATP content and kinase activities

The ATP content and kinase activities with core histones or H1 histone as substrates analysed in the roots of *V. faba* ssp. *minor* seedlings expressed in RLU per one g of FW of the apical part of roots showed that, in comparison to T0 Ctrl roots, after treatment with kinetin for 48, 72 and 96 h ATP amounts were significantly ($P < 0.05$ or $P < 0.01$) lower, by about 40, 30 and 85 %, respectively (Fig. 12a).

Kinase activities with core histones as substrate in the extracts from the roots of *V. faba* ssp. *minor* seedlings treated with kinetin for 48 h compared to T0 Ctrl were significantly ($P < 0.01$) lower by about 55 %, while in the roots treated with kinetin for 72 h, they were significantly ($P < 0.01$) greater by about 70 % and after 96 h treatment, they were significantly ($P < 0.01$) lower by about 80 % (Fig. 12b).

Activities of kinase with H1 histone as a substrate in the extracts from the roots of *V. faba* ssp. *minor* seedlings treated with kinetin for 48, 72 and 96 h as compared to T0

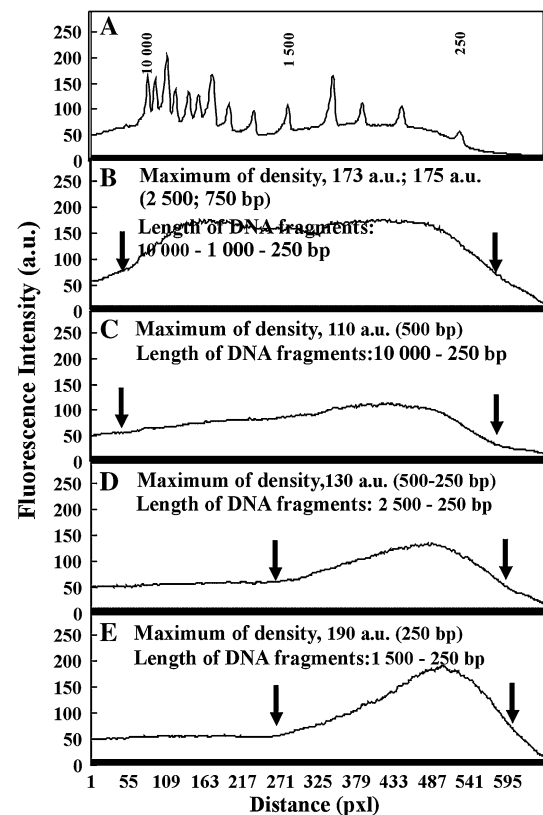


Fig. 11 Densitometric plot of fluorescence intensity of electrophoresed DNA markers (a) and faba bean DNA digested for 30 min with acidic (line b, c) and basic (line d, e) nucleases from the 2 cm apical parts of 72-h Ctrl (b, d) and 72-h kinetin-treated *V. faba* ssp. *minor* seedling (c, e) roots. Arrows indicate electrophoresed DNA fragments

Ctrl were significantly ($P < 0.05$ or $P < 0.01$) lower by about 50, 20 and 85 %, respectively (Fig. 12c).

Discussion

Scientific literature data show that endogenous plant cytokinins, such as benzylaminopurine (BAP) or zeatin, induce PCD in plant cells (Carimi et al. 2003) but not in animal ones (Berge et al. 2006; Barciszewski et al. 2007). Additionally, BAP has a dual nature and at high concentrations it induces (Carimi et al. 2003) while at low inhibits (Kobori et al. 2007) PCD. Recently, it has been observed that also kinetin, a cytokinin naturally occurring in plant and animal organisms (Barciszewski et al. 2007), induces PCD only in plant cells (Kunikowska et al. 2013a, b). Studies of the role of plant cytokinins in PCD have been carried out using two scientific models, i.e. plant cell cultures and intact plant roots in situ. In the first one, BAP (Carimi et al. 2003) while in the second kinetin (Kunikowska et al. 2013a, b) were used.

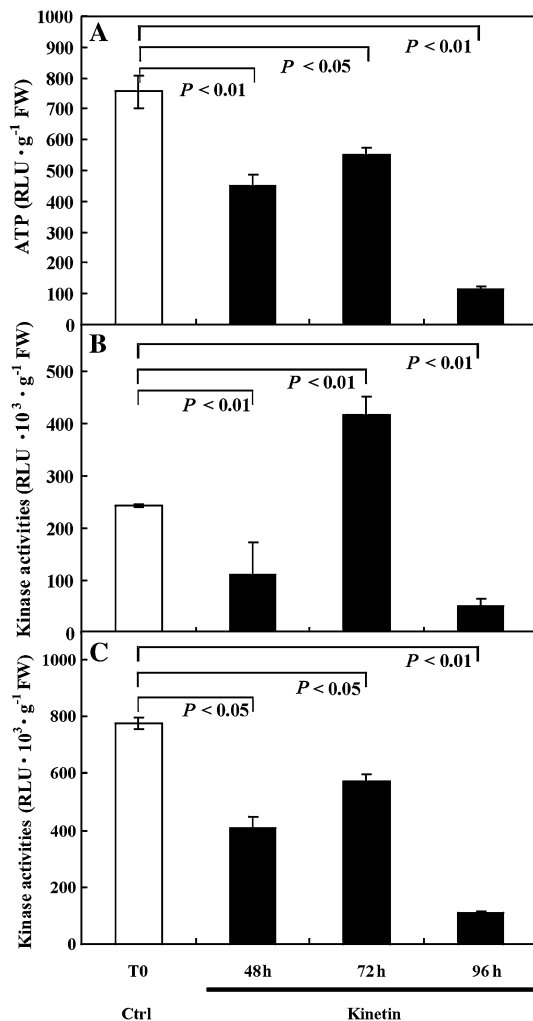


Fig. 12 ATP amount (a) and kinase activities extracted from apical parts of T0 Ctrl and of 48-, 72- and 96-h kinetin-treated *V. faba* ssp. *minor* seedling roots with core (b) and H1 (c) histones as substrates. Error bars represent the SE on the mean of three experiments ($n = 3$). $P < 0.05$ and $P < 0.01$ indicate statistically significant differences between results marked by line

In both animal and plant cells, the beginning and progress of PCD are widely studied at the nuclear level. During the programmed death, changes in nuclei reach the moment called the last step of cell death i.e. “the step beyond which the cell is irreversibly committed to die” (van Doorn 2005). This step was the aim of studies in this research. Increasing permeability of a nuclear envelope is the first metabolic hallmark of PCD (van Doorn 2005), which together with changes in permeability of mitochondrial membranes, are the most common hallmarks of PCD (Jan et al. 2008; Domínguez and Cejudo 2012).

In animals, the increasing permeability of mitochondrial membrane leads to release proapoptotic proteins (e.g. Bax, Bad) and endonuclease G (Domínguez and Cejudo 2006; Kacprzyk et al. 2011). In both plant and animal cells, cyt

c and calcium ions are released from mitochondria and they can activate specific endonucleases involved in nuclear DNA degradation (Jan et al. 2008; Kacprzyk et al. 2011; Domínguez and Cejudo 2012). Increase in the level of cellular calcium ions was observed during kinetin-induced PCD (Kunikowska et al. 2013a, b). It seems that it can activate changes in nuclease specificity what is described in this research.

Increasing permeability of a nuclear envelope can be indirectly determined by fluorescence staining using BE and OA. Due to changes in the nuclear envelope this procedure allows observer to recognise living, dying or dead cells (Byczkowska et al. 2013), and to indicate the numbers of these cells in index forms (Kunikowska et al. 2013a; Byczkowska et al. 2013).

The next stage of cell death at the nuclear level involves nuclear chromatin condensation (Jan et al. 2008; Domínguez and Cejudo 2012) which is easier to study at the morphological than the metabolic level (van Doorn 2011). Morphological changes concerning chromatin condensation during kinetin-induced PCD in root cortex cells which were presented previously (Kunikowska et al. 2013a) and they were confirmed in the present studies. They showed greater number of DAPI-stained chromocenters and higher level of fluorescence intensity of CMA₃-stained ones that were accompanied by a lower number of chromocenters. Such changes were confirmed by greater fluorescence intensity per nuclear area units of DAPI-stained and lower in CMA₃-stained chromatin. The lower fluorescence intensity per nuclear area units of the CMA₃-stained part of chromatin suggested a decondensation process as the effect of chromatin degradation in which nucleases with exo-/endonucleolytic specificity (characterised in this paper) participated. This phenomenon was reflected as a greater NPA of cortex cells of the kinetin treated seedling roots. Degradation of nuclear chromatin resulted in the appearance of nuclei containing less than 2C DNA and the formation of nuclear fragments as the effect of DNA loss from nuclei (Kunikowska et al. 2013a; Byczkowska et al. 2013) that resulted from chromatin degradation as the typical hallmark of the last step of PCD (Jan et al. 2008; van Doorn 2011; Domínguez and Cejudo 2012).

The results of the present research allowed us to explain why DNA degradation during kinetin-induced PCD in *V. faba* ssp. *minor* was not observed previously (Kunikowska et al. 2013a) as an internucleosomal process, however, such degradation was observed during PCD in other plants (Carmi et al. 2003) in which Zn²⁺- and Ca²⁺/Mg²⁺-dependent endonucleases were involved (Jan et al. 2008). Endonucleosomal and oligonucleosomal fragments form “DNA ladder” on electrophoresis gel (Jan et al. 2008; Domínguez and Cejudo 2012). Changes observed in this research which concerned the exo-/endonucleolytic specificity and activities

of both Zn^{2+} - and Mg^{2+}/Ca^{2+} -dependent nucleases against human and faba bean DNA, during kinetin-induced PCD in *V. faba* ssp. *minor* seedling roots, indicated endonucleolytic specificity of these nucleases. Moreover, DNA degradation during PCD, also those induced by kinetin (Kunikowska et al. 2013a), is a gradual, time-dependent process therefore endonucleolytic activity was masked by an exonucleolytic one. Thus the agarose gel electrophoresis of DNA extracted from the kinetin-treated *V. faba* ssp. *minor* seedling roots presented by Kunikowska et al. (2013a) did not show the DNA “ladder” reflecting internucleosomal degradation but showed “a smear” indicating exonucleolytic type of DNA degradation. It cannot be excluded that during cell death induced by kinetin faba bean nucleases also participated in chromatin condensation process similarly as in other PCD events (Jan et al. 2008; Domínguez and Cejudo 2012). Lack of DNA laddering might indicate that during cell death kinetin did not induce a specific type of nuclease similar to that known as CAD (caspase-activated DNase), the first-appearing nuclease in apoptotic animal cells responsible for the DNA internucleosomal degradation (Domínguez and Cejudo 2012).

The changes of nucleolytic specificity and greater activity of acidic nucleases from *V. faba* ssp. *minor* seedling roots expressed by line plot profile of agarose gel electrophoresis confirmed induction of the nuclear mechanism of the last step (van Doorn 2005) of nuclear degradation leading to progressive loss of chromatin and DNA content (Palavan-Unsal et al. 2005; Kunikowska et al. 2013a), it might lead to irreversible degradation of nuclei. DNA degradation was also confirmed in this research by lower actual and cytophotometrically determined DNA contents as well as DNA fragmentation. Moreover, the differences noted in specificity of nucleases extracted from the control and kinetin treated material to human and faba bean DNA indicated differences between them, although functional similarities between plant and animal nucleases induced during the PCD were reported (Jan et al. 2008; van Doorn 2011; van Doorn et al. 2011). This dissimilarity is important to understand differences between mechanisms of the animal and plant PCD, because there was research trying to explain PCD via similar approach (Carimi et al. 2003) and the apoptotic-like cell death in plants was suggested (Gladish et al. 2006). Observed type of plant cell death in which morphological changes, similar to apoptosis, is possible only in the dividing cells, i.e. in cell culture systems (Carimi et al. 2003). Similar PCD-like symptoms are reported by Gladish et al. (2006), although these studies are carried out using procambium and ground meristem of root tips.

Many processes are involved in growth and differentiation during plant development. Some of them are

controlled by methylation/demethylation processes resulting from the activity of methylase/demethylase enzymes (Jullien et al. 2006) while the others by phosphorylation/dephosphorylation processes characterised with protein kinase/phosphatase enzymes (Polit and Kaźmierczak 2007; Polit et al. 2012). The above systems belong to epigenetic mechanisms which control changes in chromatin structure (Polit and Kaźmierczak 2007; Polit et al. 2012) and gene expression (Zheng et al. 2012). Methylation/demethylation ratio of DNA is one of the epigenetic mechanisms that regulates its condensation and controls expression of genetic information during the life cycle (Jullien et al. 2006) including the cell division cycle (Brown et al. 2007). Analyses of the amount of deoxymethylcytosine in DNA of the apical parts of *V. faba* ssp. *minor* roots without meristems showed that the PCD induced by kinetin was connected with lower (after 48 h) and greater (after 72 and 96 h) levels of methylation. These temporal changes in the level of DNA methylation suggested the maintenance of level of the constant DNA methylation during kinetin-induced PCD rather than its changes. It is not clear whether the presented changes of faba bean DNA methylation resulted from constant (Jullien et al. 2006; Ovejero-Benito and Frade 2013) or variable (Zheng et al. 2012) patterns.

It also seems that the constant pattern of DNA methylation (Jullien et al. 2006) in faba bean roots might concern the cortex cells “not marked to die”. These cells play an important role in plant development similarly as same neurons in brain formation (Ovejero-Benito and Frade 2013). Such methylation might be important for faba bean root development as the changes in the pattern of DNA methylation, but not in its level, might be connected with shift of methyl groups inside GC-rich DNA or with their movement from cytosine of GC-rich DNA to adenine of AT-rich DNA. Such process might be reflected by greater AT-rich DNA condensation (observed as an enhancement of the number of DAPI-stained chromocenters and fluorescence intensity of CMA₃-stained chromocenters) and partial decondensation of GC-rich DNA (observed as a drop of the number of CMA₃-stained chromocenters probably evoking increase in the profile area of nuclei) maintaining constant DNA methylation level. Stability of the DNA methylation level might be an element of control of gene expressions in dying and/or non-dying cells that regulates mechanisms of the PCD in which DNA and other macromolecules are degraded (Zheng et al. 2012). Thus, it seems that such process should be connected with changes of DNA methylation pattern (Jullien et al. 2006). Ipso facto it cannot be excluded that if the pattern of methylation of faba bean DNA during the PCD induced by kinetin is changed, it might modify the availability of DNA sequences for specific nucleases (Domínguez and Cejudo 2012) with exo-/endonucleolytic properties. Moreover,

changes in the pattern of DNA methylation might explain the specific chromatin DNA condensation in faba bean roots, which is also one of many hallmarks of PCD (Ovejero-Benito and Frade 2013). It also might be an element of a defense mechanism of faba bean root cortex cells against death.

The present research showed that kinase activities phosphorylating H1 histone were greater while those phosphorylating core histones were lower in comparison with T0 Ctrl. On the preceding (48 h) and following (96 h) day, both kinases had lower activities than those in the roots of T0 Ctrl and 72-h kinetin-treated series. This fact together with the number of dying cells, presented in Kunikowska et al. (2013a) confirmed that the 72nd h was the climax of the cell death process induced by kinetin in faba bean root cortex cells. These results indicated that phosphorylation, like methylation of DNA, a post-translational modification of nuclear protein (Domínguez and Cejudo 2012), was also crucial for kinetin-induced PCD. It is confirmed that the scenario of nuclear degradation, which culminates programmed death of animal and plant cells (van Doorn 2005), involves chromatin condensation and then DNA and nuclear envelope degradation (Domínguez and Cejudo 2012). It seems that death of cells of faba bean roots might be connected with (1) changes in signalling of MAPK kinase activities as it was reported for PCD connected with self-incompatibility in papaver (Li et al. 2007), (2) rearrangement of chromatin condensation in which histones H2, H3 and H4 associated with lamins (as it was observed during caspase-dependent PCD; Bosch et al. 2008) and HMGA1a protein hyperphosphorylations (as it was proposed by Domínguez and Cejudo 2012) and (3) histone H1 dephosphorylation just before DNA fragmentation (Kratzmeier et al. 2000) as well as with (4) availability of DNA for nucleases and/or with (5) breakdown of the lamins connected with nuclear envelope degradation, which might be performed by kinases similar to mitotic kinases (Domínguez and Cejudo 2012). The latter phenomenon might have resulted from the fact that during apoptosis, as in mitosis, hyperphosphorylation of peripheral nucleoporin (Nup98) is observed. Disorganization of nuclear envelope by nuclear pore complexes disassembly and by nuclear envelope permeabilization preceding chromatin condensation leads to the detachment of the nuclear envelope from chromatin (Domínguez and Cejudo 2012).

The results presented in this paper on the nuclear degradation during the last step of cell death in root cortex cells of *V. faba* ssp. *minor* seedlings, including chromatin condensation, methylation and degradation of DNA as well as changes in kinase and nuclease activities are characteristic of kinetin-induced PCD. On the basis of (1) formation of lytic acidified vacuoles (Kunikowska et al. 2013a), (2) nuclear

chromatin condensation (whose nature was explained in the present research), (3) swelling of nuclei and nuclear chromatin degradation (characterised in this research), (4) nuclear envelope disassembly, (5) increase and then decrease in cell electrolyte leakage (Kunikowska et al. 2013a), and using the classification of plant cell death presented by van Doorn et al. (2011) it can be suggested that kinetin induced the vacuolar type of cell death (Kunikowska et al. 2013a). However, according to additional hallmarks of the kinetin-induced PCD, such as increase in cytosolic calcium ions (Kunikowska et al. 2013a) and ROS production (Kunikowska et al. 2013a) and ATP level depletion (data presented in this paper) as well as the fact that vacuolar type of cell death is mainly induced in cell cultures (van Doorn et al. 2011), it can be hypothesised that the kinetin-induced PCD in the root cortex cells of *V. faba* ssp. *minor* seedlings studied *in planta* resembles the autolytic type of PCD - most common during undisturbed developmental processes such as xylem, phloem and aerenchyma formation (van Doorn and Woltering 2005; van Doorn 2011) as well as during environmentally induced aerenchyma formation (Drew et al. 2000; Gunawardena 2008).

The root cortex aerenchyma formation in *V. faba* is also reported to be mediated by ethylene (Drew et al. 2000; Gunawardena 2008) and ACC (Byczkowska et al. 2013). Thus, it seems that ethylene might be the second messenger in the kinetin-induced cell death. Moreover, due to the fact that the kinetin-induced PCD is limited by the inhibitor of phosphoribosyl transferase (Kunikowska et al. 2013a), it might be suggested that after converting kinetin to corresponding monophosphates (Mlejnek and Doležel 2005), purine ligands, specific signals for cytokinin receptors (AHKs; Barciszewski et al. 2007; Caesar et al. 2011) cell death would be activated.

Overall, these results broadened our knowledge about the participation of kinetin in PCD and allowed us to propose the type of cell death induced by kinetin in root cortex cells.

Acknowledgments We thank Mrs. M. Fronczak for her help in preparing this manuscript in English and Prof. J. Barciszewski from Institute of Bioorganic Chemistry of Polish Academy of Sciences from Poznań for helpful discussion, and Mrs. E. Kuźniak-Gębarowska from Department of Physiology University of Łódź for possibility of usage Fluorescence/Luminescence Spectrophotometer F to measurements of kinase activities and ATP level.

Conflict of interest The authors declare that they have no conflict of interest.

References

- Azad AK, Ishikawa T, Sawa Y, Shibata H (2008) Intracellular energy depletion triggers programmed cell death during petal senescence in tulip. *J Exp Bot* 59:2085–2095

- Barciszewska MZ, Barciszewska AM, Rattan SIS (2007) TLC-based detection of methylated cytosine: application to aging epigenetics. *Biogerontology* 8:673–678
- Barciszewski J, Massino F, Clark BFC (2007) Kinetin—a multiactive molecule. *Int J Biol Macromol* 40:182–192
- Berge U, Kristensen P, Rattan SIS (2006) Kinetin-induced differentiation of normal human keratinocytes undergoing aging in vitro. *Ann NY Acad Sci* 1067:332–336
- Bollhöner B, Prestele J, Tuominen H (2012) Xylem cell death: emerging understanding of regulation and function. *J Exp Bot* 63:1081–1094
- Bosch M, Poulter NS, Vatovec S, Franklin-Tong VE (2008) Initiation of programmed cell death in self-incompatibility: role for cytoskeleton modifications and several caspase-like activities. *Mol Plant* 1:879–887
- Brown SE, Fraga MF, Weaver ICG, Berdasco M, Szyf M (2007) Variations in DNA methylation patterns during the cell cycle of HeLa cells. *Epigenetics* 2:54–65
- Byczkowska A, Kunikowska A, Kaźmierczak A (2013) Determination of ACC-induced cell programmed death in roots of *Vicia faba* ssp. *minor* seedlings by acridine orange and ethidium bromide staining. *Protoplasma* 250:121–128
- Caesar K, Thamm AMK, Witthöft J, Elgass K, Huppenberger P, Grefen C, Horak J, Harter K (2011) Evidence for the localization of the Arabidopsis cytokinin receptors AHK3 and AHK4 in the endoplasmic reticulum. *J Exp Bot* 62:5571–5580
- Carimi F, Zottini M, Formentin E, Terzi M, Lo Schiavo F (2003) Cytokinins: new apoptotic inducers in plants. *Planta* 216:413–421
- Domínguez F, Cejudo FJ (2006) Identification of a nuclear-localized nuclease from wheat cells undergoing programmed cell death that is able to trigger DNA fragmentation and apoptotic morphology on nuclei from human cells. *Biochem J* 397:529–536
- Domínguez F, Cejudo FJ (2012) A comparison between nuclear dismantling during plant and animal programmed cell death. *Plant Sci* 197:114–121
- Drew MC, He CJ, Morgan PW (2000) Programmed cell death and aerenchyma formation in roots. *Trends Plant Sci* 5:123–127
- Galluzzi L, Maiuri MC, Vitale I, Zischka H, Castedo M, Zitvogel L, Kroemer G (2007) Cell death modalities: classification and pathophysiological implications. *Cell Death Differ* 14:1237–1266
- Gladish DK, Xu J, Niki T (2006) Apoptosis-like programmed cell death occurs in procambium and ground meristem of pea (*Pisum sativum*) root tips exposed to sudden flooding. *Ann Bot* 97:895–902
- Gregersen PL, Holm PB, Krupinska K (2008) Leaf senescence and nutrient remobilisation in barley and wheat. *Plant Biol* 10:37–49
- Gunwardena AH (2008) Programmed cell death and tissue remodeling in plants. *J Exp Bot* 59:445–451
- Jan N, Hussain M, Andrabi KI (2008) Programmed cell death or apoptosis: do animals and plants share anything in common. *Biotechnol Mol Biol Rev* 3:111–126
- Jullien PE, Kinoshita T, Ohad N, Berger F (2006) Maintenance of DNA methylation during the *Arabidopsis* life cycle is essential for parental imprinting. *Plant Cell* 18:1360–1372
- Kacprzyk J, Daly CT, McCabe PF (2011) The botanical dance of death: programmed cell death in plants. *Adv Bot Res* 60:169–261
- Kaźmierczak A (2010) Endoreplication in *Anemia phyllitidis* coincides with the development of gametophytes and male sex. *Physiol Plant* 138:321–328
- Kobori S, Masuda Y, Horii M, Marubashi W (2007) High levels of the cytokinin BAP suppress programmed cell death in hybrid tobacco cells (*Nicotiana suaveolens* × *N. tabacum*) expressing hybrid lethality. *Plant Biotechnol* 24:375–381
- Kratzmeier M, Albig W, Hänecke K, Doenecke D (2000) Rapid dephosphorylation of H1 histones after apoptosis induction. *J Biol Chem* 275:30478–30486
- Kroemer G, Galluzzi L, Vandenabeele P, Abrams J, Alnemri ES, Baehrecke EH, Blagosklonny MV, El-Deiry WS, Golstein P, Green DR, Hengartner M, Knight RA, Kumar S, Lipton SA, Malorni W, Nuñez G, Peter ME, Tschoop J, Yuan J, Piacentini M, Zhivotovsky B, Melino G (2009) Classification of cell death: recommendations of the Nomenclature Committee on cell death. *Cell Death Differ* 16:3–11
- Kunikowska A, Byczkowska A, Kaźmierczak A (2013a) Kinetin induces cell death in root cortex cells of *Vicia faba* ssp. *minor* seedlings. *Protoplasma* 250:851–861
- Kunikowska A, Byczkowska A, Doniak M, Kaźmierczak A (2013b) Cytokinins resume: their signaling and role in programmed cell death in plants. *Plant Cell Rep* 32:771–780
- Li S, Samaj J, Franklin-Tong VE (2007) A mitogen-activated protein kinase signals to programmed cell death induced by self-incompatibility in papaver pollen. *Plant Physiol* 145:236–245
- McCall K (2010) Genetic control of necrosis—another type of programmed cell death. *Curr Opin Cell Biol* 22:882–888
- Minina EA, Filonova LH, Fukada K, Savenkov EI, Gogvadze V, Clapham D, Sanchez-Vera V, Suarez MF, Zhivotovsky B, Daniel G, Smertenko A, Bozhkov PV (2013) Autophagy and metacaspase determine the mode of cell death in plants. *J Cell Biol* 203:917–927
- Mlejnek P, Doležel P (2005) Apoptosis induced by N6-substituted derivatives of adenosine is related to intracellular accumulation of corresponding mononucleotides in HL-60 cells. *Toxicol In Vitro* 19:985–990
- Obara K, Kuriyama H, Fukuda H (2001) Direct evidence of active and rapid nuclear degradation triggered by vacuole rupture during programmed cell death in *Zinnia*. *Plant Physiol* 125:615–626
- Ovejero-Benito MC, Frade JM (2013) Brain-derived neurotrophic factor-dependent cdk1 inhibition prevents G2/M progression in differentiating tetraploid neurons. *PLoS One* 5:e64890. doi:10.1371/journal.pone.0064890
- Palavan-Unsal N, Buyuktuncer ED, Tufekci MA (2005) Programmed cell death in plants. *J Cell Mol Biol* 4:9–23
- Pennell R, Lamb C (1997) Programmed cell death in plants. *Plant Cell* 9:1157–1168
- Polit J, Kaźmierczak A (2007) Okadaic acid (1 μM) accelerates S phase and mitosis but inhibits heterochromatin replication and metaphase–anaphase transition in *Vicia faba* meristem cells. *J Exp Bot* 58:2785–2797
- Polit JT, Kaźmierczak A, Walczak-Drzewiecka A (2012) Cell cycle-dependent phosphorylation of pRb-like protein in root meristem cells of *Vicia faba*. *Protoplasma* 249:131–137
- Reape TJ, Molony EM, McCabe PF (2008) Programmed cell death in plants: distinguishing between different modes. *J Exp Bot* 59:435–444
- van Doorn WG (2005) Plant programmed cell death and the point of no return. *Trends Plant Sci* 10:478–483
- van Doorn WG (2011) Classes of programmed cell death in plants, compared to those in animals. *J Exp Bot* 62:4749–4761
- van Doorn WG, Woltering EJ (2005) Many ways to exit? Cell death categories in plants. *Trends Plant Sci* 10:117–122
- van Doorn WG, Balk PA, van Houwelingen AM, Hoerberichts FA, Hall RD, Vorst O, van der Schoot C, van Wordragen MF (2003) Gene expression during anthesis and senescence in Iris flowers. *Plant Mol Biol* 53:845–863
- van Doorn WG, Beers EP, Dangl JL, Franklin-Tong VE, Gallois P, Hara-Nishimura I, Jones AM, Kawai-Yamada M, Lam E, Mundy

J, Mur LAJ, Petersen M, Smertenko A, Taliany M, Van Breusegem F, Wolpert T, Woltering E, Zhivotovsky B, Bozhkov PV (2011) Morphological classification of plant cell deaths. *Cell Death Differ* 18:1241–1246

Zheng Z, Li L, Liu X, Wang D, Tu B, Wang L, Wang H, Zhu W (2012) 5-Aza-2-deoxycytidine reactivates gene expression via degradation of pRb pocket proteins. *FASEB J* 26:449–459